



Optimum polarization configuration of planar circular patch MIMO antenna

Rina Pudji Astuti^{1*}, Eva Lucky Wijaya², Trasma Yunita³, Harfan Hian Ryanu⁴
^{1,2,3,4}School of Electrical Engineering, Telkom University
^{1,2,3,4}Jl. Terusan Buah Batu Dayeuhkolot Bandung, 40257, Indonesia
*Corresponding email: rinapudjiastuti@telkomuniversity.ac.id

Received 22 Desember 2021, Revised 01 January 2022, Accepted 26 February 2022

Abstract —A novel four-element Multiple Input Multiple Output (MIMO) with unique polarization arrangement and high isolation between elements is presented in this paper. First, a truncated edge method is used to obtain a single antenna with circular polarization. Then by positioning the feed point at a certain location, Right-Hand Circular Polarization (RHCP) or Left-Hand Circular Polarization (LHCP) is obtained for a single antenna. After that, four elements of these antennas are arranged with several polarization configurations both in Co-Polarization and Cross-Polarization. Both simulation and measurement results showed that MIMO with Co-Polarization has a slightly wider bandwidth equal to 295.25 MHz than cross-polarization with a bandwidth of 274.63 MHz, due to better return loss performed by the former. However, from the mutual coupling perspective, it is observed that MIMO with Cross-Polarization can reduce the mutual coupling from -17.6676dB into -22.462 dB compared to Co-Polarization with the same element distance.

Keywords – MIMO, circular polarization antenna, cross-polarization, 5G

Copyright © 2022 JURNAL INFOTEL

All rights reserved.

I. INTRODUCTION

The rapid development of many areas triggers increasingly high demand speed of Internet access. 5G (fifth generation) wireless communication is one of the technologies that can provide high-speed Internet service. The technology is planned to be implemented in 2020 in Indonesia. 5G is expected to support data rates of up to 10 Gbps for uplink and 20 Gbps for downlink, latency values less than 1 ms, high reliability, and stable connectivity [1]. Such performance is supported by the multiple antenna distribution arranged linearly, cylindrically, and in planar configuration [2]–[5]. In addition, the planar shape antenna arrangement is easier to install on a flat surface of the building [6].

5G communication was recommended on several frequency spectrums candidates capable of delivering wide coverage and supporting a large number of users. The frequency allocation candidate for 5G is Sub-1 GHz, 1-6 GHz, and above 6 GHz. The frequency range 1-6 GHz offers good coverage and capacity advantages. The spectrum range 3.3-3.8 GHz is frequency operation of many 5G services [7], [8].

5G technology adopts the MIMO system usage on its antenna to obtain the specification previously mentioned. MIMO (Multiple Input Multiple Output) antenna systems utilize more than one antenna on the transmitter side and the receiver side to increase the channel capacity without increasing bandwidth and power [9]. Regarding several previous research [10]–[12], it was discussed and studied that the performance of a MIMO antenna system is influenced by the number of antennas and antenna characteristics and its array configuration. Therefore, coupling is an important aspect that needs consideration in MIMO antenna design. Furthermore, the antenna polarization on each MIMO element also influences the mutual coupling between antenna elements. Configuring a certain polarization of antenna elements is considered an attempt to reduce the mutual coupling value in the MIMO system [13]–[15].

One of the methods used to reduce mutual coupling is by using a polarization conversion isolator [13], decoupling ground [14], or electromagnetic bandgap (EBG) [15]. However, all those mentioned methods require additional components between radiating elements that increase the antenna's overall size. This

paper performed a study on polarization configuration in MIMO antenna without using additional elements. The case study at the 5G spectrum at a frequency range of 3.3 GHz to 3.8 GHz was carried out to analyze the polarization arrangement of the circular patch elements of the planar MIMO antenna. A truncated method is elaborated to obtain a circular polarization property of the antenna. The feed point selection is used to adjust the circular polarization type both as the right hand and left hand.

The MIMO microstrip antenna system needs to determine proper polarization arrangement to produce the optimal MIMO antenna performance. In this paper, an investigation of the MIMO antenna polarization arrangement effect has been conducted with Co-Polarization configurations and Cross-Polarization, which are arranged in the field against the mutual coupling and the channel capacity for 5G communication.

The discussion on this paper was organized as follows. Section I elaborates the background and problems in the paper. Then in Section II, there is a MIMO antenna design with a circular patch element compiled with several polarizing configurations to obtain the optimum MIMO arrangement. Section III discusses the number of results obtained, while Section IV shows the analysis of the mentioned results. Finally, section V is the conclusion

II. RESEARCH METHODS

A. Circular Polarization Patch Antenna

In this study, the circular-shaped patch element was selected as a MIMO antenna element that easily regulates the type of polarization by adjusting the location of the feeding point. For the circular patch microstrip antenna, several formulas are used to determine the dimension of the antenna [16]. The radius of the patch can be calculated using (1), with h is the substrate thickness, ϵ_r is the relative dielectric permittivity of substrates f_r is the frequency of the resonance antenna, and a can be determined by using (2) and (3)[17].

$$r = a \left\{ 1 + \frac{2h}{\pi a \epsilon_r} \left[\ln \left(\frac{\pi a}{2h} \right) + 1,7726 \right] \right\}^{\frac{1}{2}} \quad (1)$$

$$a = \frac{F}{\left\{ 1 + \frac{2h}{\pi \epsilon_r F} \left[\ln \left(\frac{\pi F}{2h} \right) + 1,7726 \right] \right\}^{\frac{1}{2}}} \quad (2)$$

$$F = \frac{8.791 \times 10^9}{f_r \sqrt{\epsilon_r}} \quad (3)$$

The substrate thickness is determined from the material used to realize the antenna. In this design, the RF-4 (Epoxy) substrate is used and generally has a thickness of 1.6 mm. While on the patch and ground plane, the copper material has a thickness of 0.035 mm. The minimum dimensions of the ground plane and substrate can be calculated using the following equation in (4-5) [18], with W and L are approached with a diameter of the patch ($2r$)

$$W_g = 6h + W \quad (4)$$

$$L_g = 6h + L \quad (5)$$

As shown in Fig. 1, the coaxial probe's technique is used to connect antennas with excited signal sources. This technique is chosen because it is easier to determine the feeding point, which is then used to determine antenna polarization. Input impedance and polarization adjustment of the antenna can be performed by placing a feed point at a certain position on the antenna patch [18].

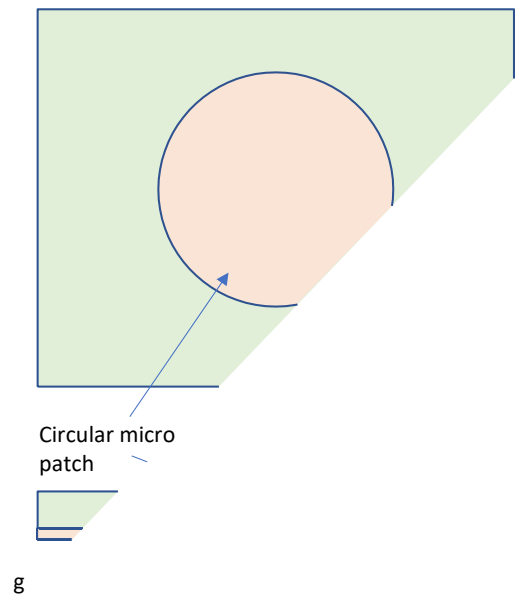


Fig.1. Coaxial Probe technique.

Truncated edge is applied to produce circular polarization on the used antennas. For example, a truncated patch with an angle of 135° or 315° slope, as shown in Fig 2, will cause surface currents to spin over the patch and produce LHCP or RHCP polarization [18].

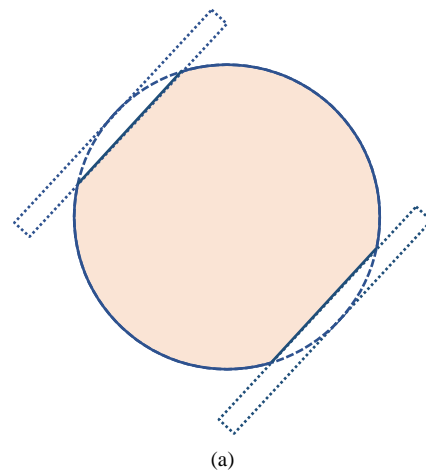


Fig. 2. Truncated edge at Circular Patch Antenna

The truncated edge method on the circular patch adopts the truncated corner method performed on a rectangular patch to obtain the circular polarization.

The corner truncated of a rectangular patch with equilateral triangle forms can be determined using the calculations (6-8) [19].

$$s = \sqrt{\Delta S}, \tag{6}$$

ΔS is the area of antenna angle intersection and calculated with the following equation.

$$\frac{\Delta S}{W} = \frac{1}{2Q} \tag{7}$$

W is the width or diameter of the antenna, while Q is a quality factor of the antenna. Moreover, the antenna quality factor can be determined using (8).

$$Q = \frac{f_0}{BW_n}. \tag{8}$$

f_0 is the center frequency operation of the antenna and BW_n is the antenna bandwidth. From the above formulas, there is an equation that can be used to calculate the value of s directly, as written in (9).

$$s = \sqrt{\frac{W}{Q}} \tag{9}$$

Where W is the width or diameter of the antenna, while Q is a factor of quality that is owned by an antenna.

In the circular microstrip patch antenna design, the copper material with a thickness of 0.035 mm is used as the patch and ground plane material. Meanwhile, the substrate is using the RF-4 Epoxy material that has a thickness of 1.6 mm, and $\epsilon_r = 4.3$. The selection of substrate material is based on the properties of the RF-4 Epoxy substrate, which has a moderate thickness, dielectric constant, and is relatively cheap to produce the antennas with wide bandwidth. Table 1 shows the specifications of a single circular patch microstrip antenna designed.

Table 1. Specification of Single Patch.

Specification	Description
Patch shape	circular
Return Loss	≤ -10 dB
Axial Ratio	≤ 3 dB at a whole bandwidth
Polarization	LHCP/RHCP
Frequency range	3,3 GHz – 3,8 GHz

The circular patch dimension calculation is started by determining the antenna's resonant frequency. In this research, a case study was carried out on designing the MIMO antenna for 5G at a frequency of 3.5 GHz. So, using 3.5 GHz as the resonance frequency (f_r), and the substrate data, the radius of the circular patch (r) can be determined using (1-3). Then the substrate and ground plane dimensions (l_g and w_g) are determined based on (4-5). The dimensions of the circular patch are then listed in Table 2.

Table 2. Calculation Results of the Antenna Dimension.

Parameter	Description	Value (mm)
h	Dielectric thickness	1,6
t	Conductor thickness	0,035
r	Patch radius	12,125
w_g	Groundplane width	36,658
l_g	Groundplane length	36,658

The next step is to perform a computer simulation with the corresponding antenna dimensions in Table 2. Based on the quality factor obtained from the simulation result, the truncated part on the antenna patch with the truncated edge technique can be determined. Truncated field calculations are obtained using (7). On the RHCP single patch antenna, a port point placement is found on the y-axis for $x = 0$, as shown in Fig.3.

Table 3. Optimized Result of Single Patch Dimension

Parameter	Description	Value (mm)
h	Dielectric thickness	1,6
t	Conductor thickness	0,035
r	Patch radius	11,75
w_g	Ground plane width	33,86
l_g	Ground plane length	33,86
s	Truncated edge size	0,949

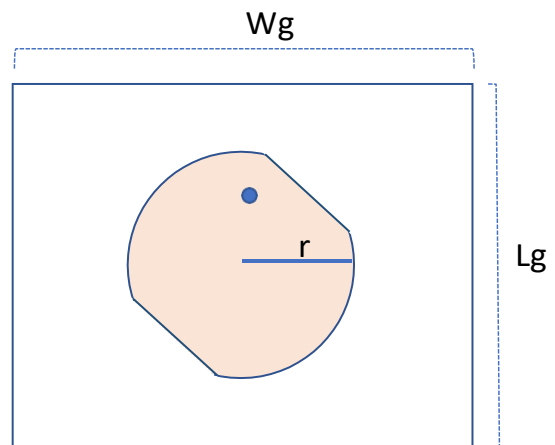


Fig. 3. Circular patch antenna dimension with RHCP.

The simulations were performed using a 3D Modeler software based on the antenna dimension listed in Table 3. The obtained result on the return loss is depicted in Figure 4. It can be seen on the result that the lowest return loss value is at a frequency of 3.586 GHz, with a return loss of -27.419348 dB. Antennas have a return loss value below -10 dB starting from 3.3308 GHz to 3.6674 GHz.

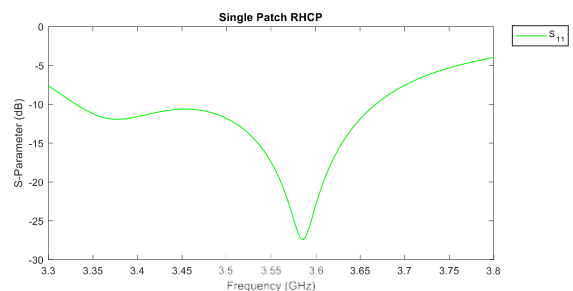


Fig. 4. Return Loss of single patch with RHCP.

The antenna radiation pattern is shown in Fig.5, and the result indicates that the maximum direction is

perpendicular to the patch plane with a beamwidth value of 97° . The axial ratio is observed at the maximum direction, and the result is shown in Fig. 6. For the lowest axial-ratio value that meets the antenna's working range frequency, it is at a frequency of 3.435 GHz with an axial ratio of 0.11155267 dB on $\phi = 0$, as seen in Fig.6. Meanwhile, to determine the type of polarization RHCP can be seen using the distribution current at the patch surface which describes a rotation direction. The RHCP polarization type can be seen from the direction of the rotation that is counterclockwise (CCW), as shown in Fig.7. It is indicated by black arrow on upper left corner of image appears rotated to the left.

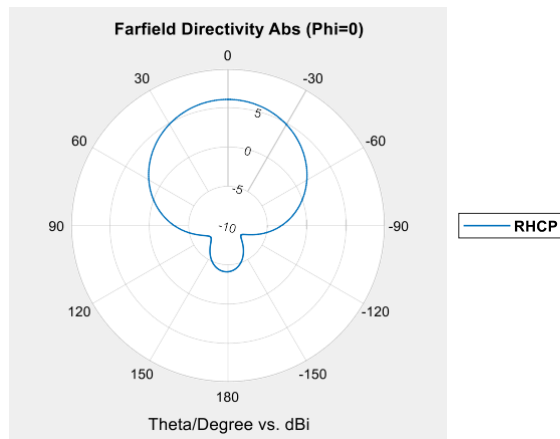


Fig. 5. Farfield polar plot of RHCP.

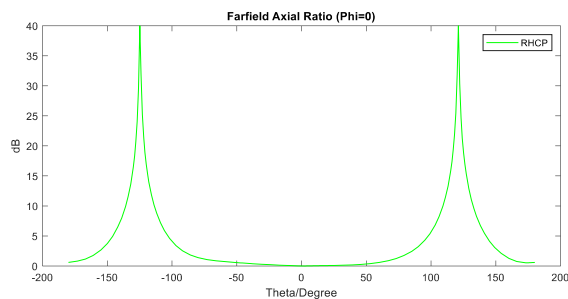


Fig. 6. Farfield Axial Ratio Cartesian of RHCP.



Fig. 7. The direction of the Rotation is Shown as RHCP Polarization.

In addition to observing the direction of the current rotation, the type of polarization between RHCP and LHCP in simulation results can also be determined from which one has a larger directivity value. For example, in RHCP single patch antenna, the directivity data were obtained at a frequency of 3.435 GHz with a value of 6.049 dBi for the Right Polarization. At the same time, it only had a directivity value of -57.798 dBi for Left Polarization. Thus, it can be concluded that the single patch antenna simulated has Right Hand Circular Polarization (RHCP).

In a single patch antenna simulation with Right Hand Circular Polarization, the axial ratio bandwidth for circular polarization is 65.5 MHz, located at a frequency range of 3.3925 GHz to 3.458 GHz. The bandwidth value of the circular polarization axial ratio is compared with the return loss bandwidth, which has a value of 0.196%. So it can be stated that a single patch antenna RHCP with a bandwidth impedance of 333.99 MHz has 0.196% of its frequency range that generates a circular polarization wave.

A single patch antenna with LHCP is obtained by placing the coordinate of the feed point on the x-axis for $y = 0$ as in Figure 8.

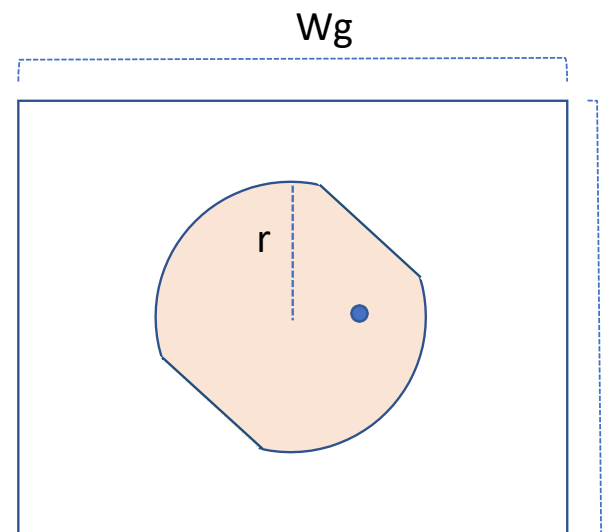


Fig. 8. Single Patch LHCP antenna.

The antenna radiation pattern is shown in Fig.10, and the result indicates that the maximum direction is perpendicular to the plane with a beamwidth value of 97.3° . The axial ratio is observed at the maximum direction and the result is shown in Fig. 6. The lowest axial ratio is at a frequency of 3.435 GHz with an axial ratio of 0.0092366876 dB on $\phi = 0$, as seen in Fig.11. Meanwhile, the type of polarization can be observed using the distribution current at the patch surface, which describes a rotation direction. The LHCP polarization type can be seen from the direction of the rotation that is clockwise (CW), as shown in Fig.12. It is indicated by black arrow on upper left corner of image appears rotated to the right.

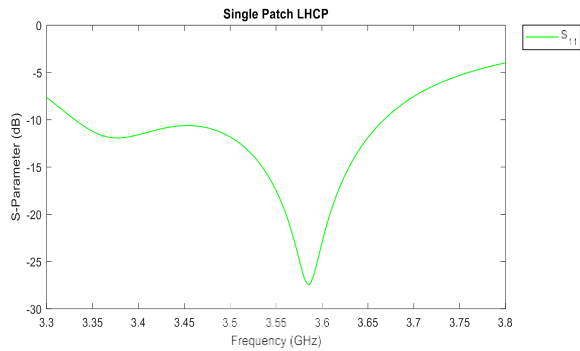


Fig. 9. Return Loss single patch LHCP Graph.

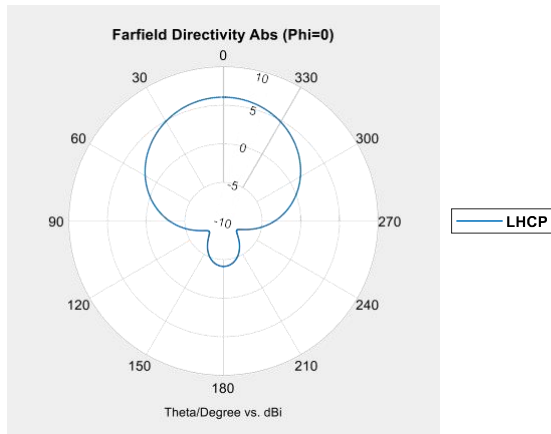


Fig. 10. Farfield polar plot of LHCP

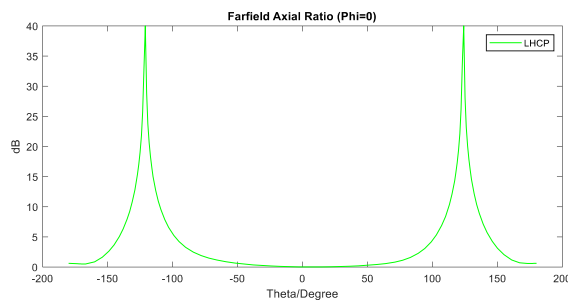


Fig. 11. Farfield Axial Ratio Cartesian plot of LHCP

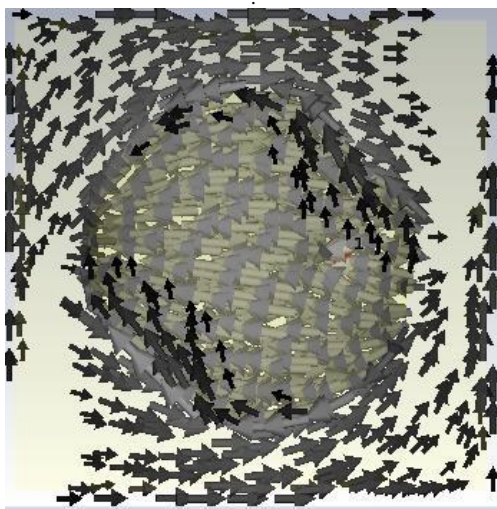


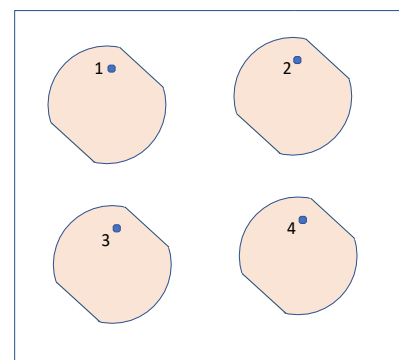
Fig. 12. The direction of the Rotation is Shown as LHCP Polarization

The Left Polarization directivity value larger than the Right Polarization. The directivity for LHCP direction at 3.435 GHz is 6.011 dBi, while for RHCP direction is only -53.914 dBi. Thus, it can be concluded that the single antenna simulated has a Left-Hand Circular Polarization (LHCP). The axial ratio bandwidth of LHCP simulation is 66 MHz within the working frequency 3.3925 GHz – 3.4585 GHz, which, if compared with the return loss bandwidth, has a value of 0.197%.

B. MIMO Antenna with Co and Cross Polarized Configuration

After designing a single patch microstrip antenna with Right Hand Circular Polarization and Left-Hand Circular Polarization, the MIMO antenna design was conducted, consisting of 4 single patch antenna elements. The distance between the elements is determined by a half wavelength of resonances frequency ($d = \frac{\lambda_{er}}{2}$) with $\lambda_{er} = \frac{\lambda_0}{\sqrt{\epsilon_r}}$. Thus, the minimum distance between antennas is 26.68 mm. Furthermore, the distance is optimized into 34 mm to obtain the S-Parameter values that meet the desired specifications, which are under -10 dB for the return loss value, and below -20 dB for the mutual coupling value[20], [21].

This research investigated two types of polarization configuration in the MIMO antenna. The first polarization configuration composes four single CP patch elements into the MIMO antenna with Co-Polarization, and the second polarizing configuration composes the antenna with the Cross-Polarization configuration. The two types of polarization configuration of four-element MIMO antenna are depicted in Fig 13 and 14.



(a)

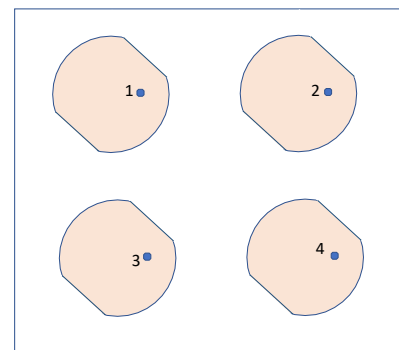


Fig. 13. MIMO Co-Polarization Antenna (a) RHCP (b) LHCP

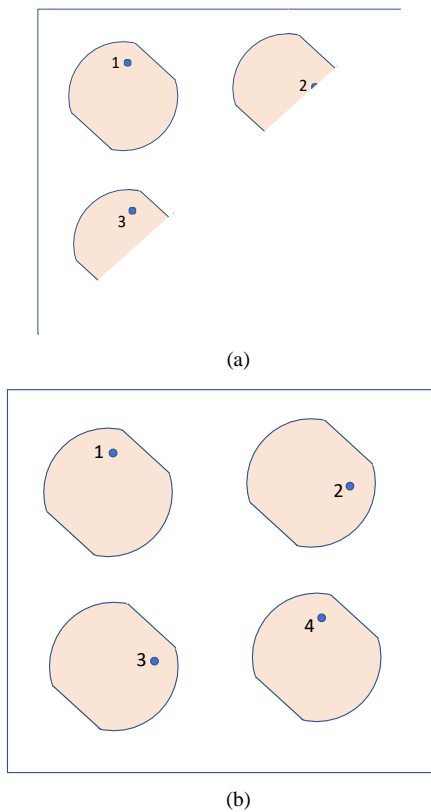
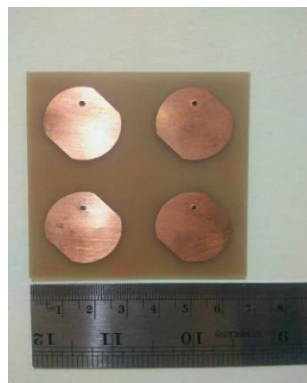


Fig. 14. MIMO Cross-Polarization Antenna (a) R-L-R-L and (b) R-L-L-R



(a)



Fig. 15. Realization Result. (a) Co-Polarization MIMO; (b) Cross-Polarization MIMO.

III. RESULTS

Laboratory measurements were performed to validate the previously obtained results. The MIMO antenna with several configurations depicted in Fig. 13 dan 14 was fabricated for laboratory measurement. The fabrication result of the MIMO antennas is shown in Fig 15. The phase difference measurement was conducted to prove the presence of RHCP or LHCP polarization on the designed antennas. The phase measurement performed by placing an antenna transmitter, and a dipole antenna as receiver. The observation data analyzed is at a frequency of 3.435 GHz. The obtained phase measurement data is then reported in Table 4. The results indicate that element 1 and element 2 are proven the LHCP and RHCP.

Table 4. Measurement Result.

Antenna Element	Vertical Phase	Horizontal Phase	Phase Difference	Description
Element 1	4,67°	-57,26°	-52,59°	LHCP
Element 2	-64,54°	-142,42°	77,88°	RHCP

A. Co-Polarized Configuration

The S-Parameters comparison between simulation and measurement result for the Co-Polarized configuration is shown in Fig 16. From this result, we can see a slight discrepancy between simulation and the measurements result due to the accuracy of the fabrication. The comparison result is also summarized in Table 5. The highlight of the green color illustrates the lower S-Parameter value, whereas the orange color illustrates the higher S-Parameter value.

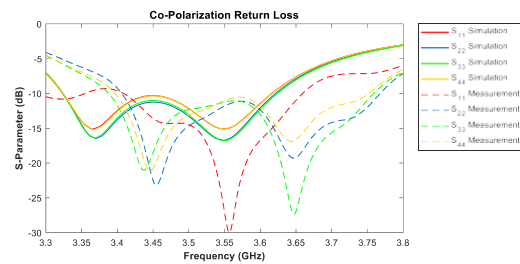


Fig. 16. Return Loss Between Simulation and Measurement

Table 5. S-Parameter Differences Between Simulation and Measurement for Co-Polarization Configuration

Parameter	Simulation (dB)	Measurement (dB)
S11	-11.832	-14.272
S22	-12.889	-14.980
S33	-12.679	-12.488
S44	-11.844	-13.352
S12	-17.683	-21.950
S13	-37.900	-18.405
S14	-36.842	-26.923
S21	-17.679	-22.591
S23	-24.093	-26.935
S24	-37.345	-16.948

Parameter	Simulation (dB)	Measurement (dB)
S31	-37.801	-18.946
S32	-24.093	-27.533
S34	-17.684	-21.395
S41	-36.886	-27.420
S42	-37.345	-16.761
S43	-17.684	-21.167

In addition, from the bandwidth comparison between simulation and fabrication in Table 6, a slight difference in bandwidth can be observed. However, the overall result shows that the measured impedance bandwidth was greater than the simulation.

Table 6. Bandwidth Differences Between Simulation and Measurement for Co-Polarization Configuration

Parameter	Co-Polarization Simulation (dB)	Co-Polarization Measurement (dB)
BW Patch 1	0.292 GHz	0.304 GHz
BW Patch 2	0.297 GHz	0.3615 GHz
BW Patch 3	0.2995 GHz	0.37 GHz
BW Patch 4	0.2925 GHz	0.354 GHz
Average BW	0.295250118 GHz	0.347375 GHz

B. Cross-Polarization Configuration

Comparison of simulated results and measurements for cross-polarization configurations are shown in Figure 17. From this result, we can see a slight discrepancy between simulation and the measurements due to the fabrication process's accuracy. The S-Parameter plot in Fig 17 shows a frequency shift towards the right when comparing the measured result with the simulation result. The comparison result is also summarized in Table 7. The difference evaluation of S-Parameter simulation results and the measurement has been performed at the frequency point 3.357 GHz. The highlight of the green color illustrates the lower S-Parameter value, whereas the orange color illustrates the higher S-Parameter value.

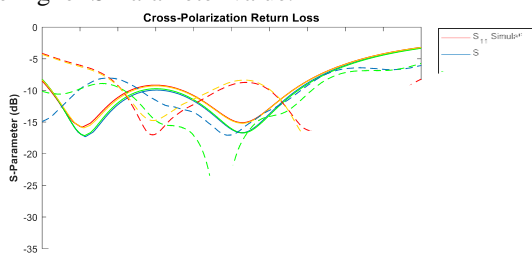


Fig. 17 Return Loss Between Simulation and Measurement for Cross-Polarization

Table 7. S-Parameter Differences Between Simulation and Measurement for Co-Polarization Configuration

Parameter	Simulation (dB)	Measurement (dB)
S11	-15.6717	-16.44407
S22	-17.2945	-18.97
S33	-17.134	-18.8481
S44	-15.8863	-16.58
S12	-22.0532	-24.7245
S13	-21.9221	-23.9226
S14	-21.908	-23.8862
S21	-22.0913	-24.7467

Parameter	Simulation (dB)	Measurement (dB)
S23	-35.6467	-33.2397
S24	-20.2737	-22.2364
S31	-21.9223	-23.8072
S32	-35.6399	-33.8229
S34	-20.5251	-23.0511
S41	-21.9069	-23.1167
S42	-20.2734	-22.7371
S43	-20.5578	-23.6379

There is a difference in return loss value and mutual coupling between the simulation result and the result of antenna measurement due to the frequency shifting that occurs during the measurement process. The dielectric constant difference values cause frequency shifting. of the simulated antenna substrate and the measurement result of the fabrication antenna. As well as the difference in the point of the simulation and fabrication results, the impedance value is on the fabrication result antenna is different from the simulation results. However, the average value shows better results on the mutual coupling data of the measurement results. Table 7 shows the bandwidth value of the MIMO cross-polarization antenna for both measurement and simulation.

Table 8. Bandwidth Differences Between Simulation and Measurement for Cross-Polarization Configuration

Parameter	Cross-Polarization Simulation (dB)	Cross-Polarization Measurement (dB)
BW Patch 1	0.2495 GHz	0.3025 GHz
BW Patch 2	0.3055 GHz	0.259 GHz
BW Patch 3	0.2885 GHz	0.2915 GHz
BW Patch 4	0.255 GHz	0.2945 GHz
Rata-rata BW	0.274625003 GHz	0.286875 GHz

According to Table 8, we can find that on the MIMO cross-polarization antenna, neither the simulation nor the measurements indicate the greater bandwidth value than the MIMO co-polarization antenna both in simulation and measurement. This condition is due to the average return-loss of graphs on the MIMO co-polarization antenna showing better results. However, although the MIMO Co-Polarization antenna return loss is better than Cross-Polarization, it could be observed from the mutual coupling. The MIMO Cross Polarization antenna shows better results, as all mutual coupling values meet the specification results, i.e., smaller than -20 dB.

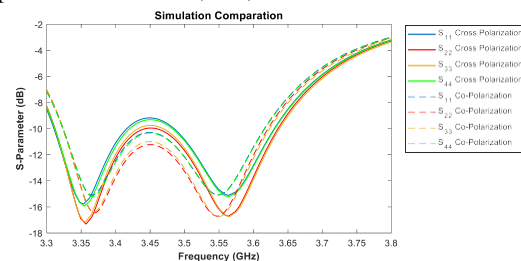


Fig. 18 Return Loss Simulation Comparison Between Co-Polarization and Cross-Polarization

IV. DISCUSSION

Polarization arrangement on MIMO antenna elements in Co-polarized and Cross-Polarized configuration aims to compare the results obtained from these two polarization settings against the reviewed S-parameters, including return loss and mutual coupling. Based on the Return loss result in Figure 18, it is revealed that the return loss value on the MIMO antenna of simulated results for co-polarization configurations has lower values, as all values are below -10 dB. The value of the return loss affects a large bandwidth.

Table 9. Bandwidth Comparison Between Co-Polarization and Cross-Polarization Simulation

Parameter	Co-Polarization Simulation	Cross-Polarization Simulation
BW Patch 1	0.292 GHz	0.2495 GHz
BW Patch 2	0.297 GHz	0.3055 GHz
BW Patch 3	0.2995 GHz	0.2885 GHz
BW Patch 4	0.2925 GHz	0.255 GHz
Average BW	0.295250118 GHz	0.274625003 GHz

The measurement result shown in Fig. 19 and Table 10 that Co- Polarized configuration has larger bandwidth than the Cross Polarized configuration.

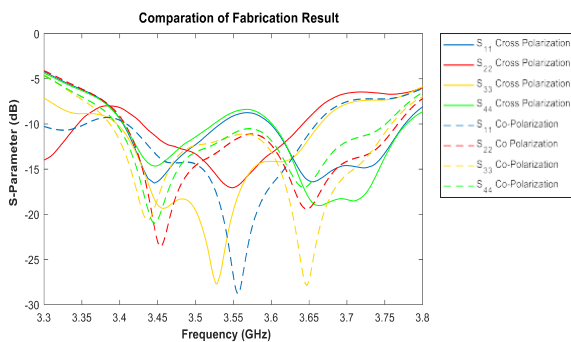


Fig. 19 Return Loss Measurement Comparison Between Co-Polarization and Cross-Polarization.

Table 10 Bandwidth Comparison Between Co-Polarization dan Cross-Polarization MIMO Measurement

Parameter	Co-Polarization Simulation	Cross-Polarization Simulation
BW Patch 1	0.304 GHz	0.3025 GHz
BW Patch 2	0.3615 GHz	0.259 GHz
BW Patch 3	0.37 GHz	0.2915 GHz
BW Patch 4	0.354 GHz	0.2945 GHz
Average BW	0.347375 GHz	0.286875 GHz

In addition to the return loss value, the MIMO Co-Polarization and Cross-Polarization antennas also experience differences in the mutual coupling value. In Figure 20, it can be seen that the value of S21 for the Co-Polarization had a value of -17.6676 dB at 3.5 GHz, whereas for cross-polarization MIMO antenna had a value of -22.462 dB. In line with S21, the S31 for Co-Polarization configuration at the frequency of 3.4 GHz is also smaller than Cross-Polarization, which is -17.9104 dB, and -22.8574 dB, respectively. Both

results confirm that the Cross-Polarization configurations have better mutual coupling than Co-polarized configurations.

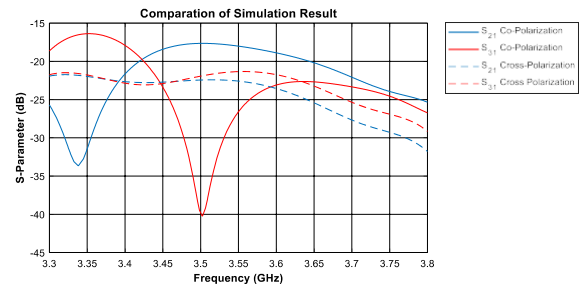


Fig. 20 Simulated Mutual Coupling Antenna.

From the measurement result shown in Figure 21, it could be seen that S21 Co-Polarization has better mutual coupling compared to Cross-Polarization at -45dB and -39 dB, respectively. However, it could be seen that not all mutual coupling values in bandwidth observed for Co-Polarization Antenna meet the specification results of -20dB, while for Cross-Polarization has a mutual coupling below -20dB in all observed bandwidth.

The comparison of radiation patterns aims to determine the difference in the effect of polarization arrangement on the MIMO antenna against the transmission beam direction formed by the antenna. Fig 22 and 23 shows radiation patterns formed by each polarizing configuration on the MIMO antenna. The Co-Polarized and Cross-Polarized configuration have relatively the same radiation pattern. This is because both configurations have a directional pattern. It means that the polarization arrangement has no significant influence on the radiation pattern.

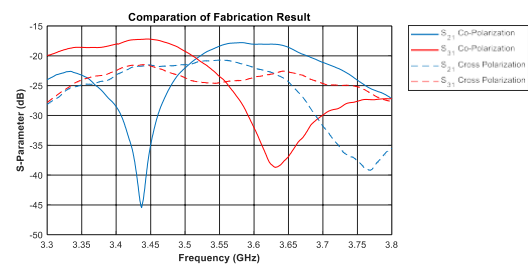


Fig. 21 Measured Mutual Coupling Antenna.

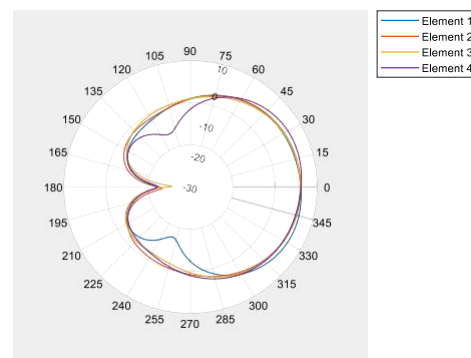


Fig. 22 Radiation Pattern for Co-Polarization MIMO

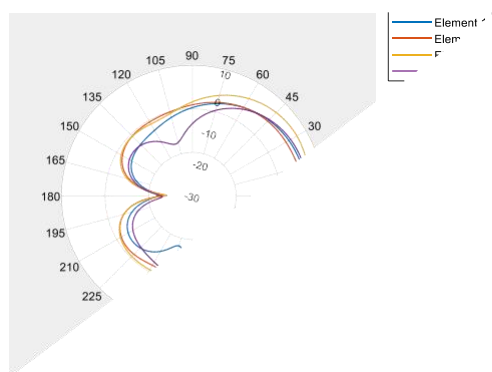


Fig. 23 Radiation Pattern for Cross-Polarization MIMO

V. CONCLUSION

The studies of polarization arrangement in planar MIMO antenna with circular patch element were performed in this paper. A 3.5 GHz circular polarized planar MIMO antenna was taken for investigation. The polarizing arrangement using the Cross-Polarization method configuration can lower the mutual coupling value of the MIMO antenna coupling elements and the return loss value on the antenna elements. Taking a distance of 34 mm between adjacent elements, the Cross-Polarization method gives a lower mutual coupling value equal to -22.462 dB than Co-Polarization which only has a value of -17.6676 dB. Therefore, polarization arrangement can be used to increase the capacity of the MIMO system. The polarization arrangement should pay attention to the value of return loss occurring on each antenna element. After all, the impedance matrix formation on the transmitter or receiver side requires the entire component S-Parameter on the antenna consisting of return loss mutual coupling.

REFERENCES

- [1] M. Fuentes *et al.*, "5G New Radio Evaluation Against IMT-2020 Key Performance Indicators," *IEEE Access*, vol. 8, p. 110896, Dec. 2020, doi: 10.1109/ACCESS.2020.3001641.
- [2] K. A.S., L. N., and B. Syihabuddin, "Perancangan Antena MIMO 2x2 Array Rectangular Patch dengan U-Slot untuk Aplikasi 5G," *Jurnal Nasional Teknik Elektro dan Teknologi Informasi (JNTETI)*, vol. 6, Dec. 2017, doi: 10.22146/jnteti.v6i1.299.
- [3] Gautam Rai, "A Survey: Antenna Design Structure for Massive MIMO," *International Journal of Advanced and Innovative Research*, vol. 7, no. 2, pp. 79–81, 2018.
- [4] J. Guo, F. Liu, L. Zhao, Y. Yin, G.-L. Huang, and Y. Li, "Meta-Surface Antenna Array Decoupling Designs for Two Linear Polarized Antennas Coupled in H-plane and E-Plane," *IEEE Access*, vol. 7, pp. 100442–100452, 2019, doi: 10.1109/ACCESS.2019.2930687.
- [5] N. Wu, F. Zhu, and Q. Liang, "Evaluating Spatial Resolution and Channel Capacity of Sparse Cylindrical Arrays for Massive MIMO," *IEEE Access*, vol. 5, pp. 23994–24003, 2017, doi: 10.1109/ACCESS.2017.2763599.
- [6] U. Devi, R. Koosam, M. Venna, and B. Thota, "FOUR ELEMENT SQUARE PATCH MIMO ANTENNA FOR DSRC, WLAN, AND X-BAND APPLICATIONS," *Progress In Electromagnetics Research M*, vol. 100, pp. 175–186, Dec. 2021, doi: 10.2528/PIERM20103101.
- [7] Y. Chen, Q. Liu, Y. Zhang, H. Li, and W. Zong, "Design of a Compact Base Station Antenna for 5G N78-Band Application," Dec. 2020, pp. 229–231, doi: 10.1109/ICEICT51264.2020.9334286.
- [8] C.-Y.-D. Sim, H.-Y. Liu, and C.-J. Huang, "Wideband MIMO Antenna Array Design for Future Mobile Devices Operating in the 5G NR Frequency Bands n77/n78/n79 and LTE Band 46," *IEEE Antennas and Wireless Propagation Letters*, vol. 19, no. 1, pp. 74–78, 2020, doi: 10.1109/LAWP.2019.2953334.
- [9] A. Admaja, "Kajian Awal 5G Indonesia (5G Indonesia Early Preview)," *Buletin Pos dan Telekomunikasi*, vol. 13, p. 97, Dec. 2015, doi: 10.17933/bpostel.2015.130201.
- [10] J. W. Wallace and M. A. Jensen, "Mutual coupling in MIMO wireless systems: a rigorous network theory analysis," *IEEE Transactions on Wireless Communications*, vol. 3, no. 4, pp. 1317–1325, 2004, doi: 10.1109/TWC.2004.830854.
- [11] X. Li and Z.-P. Nie, "Mutual coupling effects on the performance of MIMO wireless channels," *IEEE Antennas and Wireless Propagation Letters*, vol. 3, pp. 344–347, 2004, doi: 10.1109/LAWP.2004.840252.
- [12] Y. Yu, J. Zhang, P. J. Smith, and P. A. Dmochowski, "Theoretical Analysis of 3-D Channel Spatial Correlation and Capacity," *IEEE Communications Letters*, vol. 22, no. 2, pp. 420–423, 2018, doi: 10.1109/LCOMM.2017.2765307.
- [13] Y.-F. Cheng, X. Ding, W. Shao, and B.-Z. Wang, "Reduction of Mutual Coupling Between Patch Antennas Using a Polarization-Conversion Isolator," *IEEE Antennas and Wireless Propagation Letters*, vol. 16, pp. 1257–1260, 2017, doi: 10.1109/LAWP.2016.2631621.
- [14] S. Zhang, X. Chen, and G. F. Pedersen, "Mutual Coupling Suppression With Decoupling Ground for Massive MIMO Antenna Arrays," *IEEE Transactions on Vehicular Technology*, vol. 68, no. 8, pp. 7273–7282, 2019, doi: 10.1109/TVT.2019.2923338.

- [15] Y. Liu, X. Yang, Y. Jia, and Y. J. Guo, "A Low Correlation and Mutual Coupling MIMO Antenna," *IEEE Access*, vol. 7, pp. 127384–127392, 2019, doi: 10.1109/ACCESS.2019.2939270.
- [16] I. Budi, E. Nugraha, and A. Agung, "Perancangan Dan Analisis Antena Mikrostrip Mimo Circular Pada Frekuensi 2.35 GHz Untuk Aplikasi LTE," *JURNAL INFOTEL*, vol. 9, p. 136, Dec. 2017, doi: 10.20895/infotel.v9i1.130.
- [17] Constantine A. Balanis, *Antenna Theory: Analysis and Design*, 3rd ed. Canada: John Wiley & Sons, 2005.
- [18] F. Heryanto, H. Wijanto, A. D. Prasetyo, and Edwar, "Slotted patch and truncated edge techniques on microstrip antenna for CP-SAR S-band data transmitter," in *2018 International Conference on Signals and Systems (ICSigSys)*, 2018, pp. 219–223. doi: 10.1109/ICSIGSYS.2018.8372670.
- [19] R. Sainati, *CAD of microstrip antennas for wireless applications*. Norwood, Massachusetts: Artech House, Inc., 1996.
- [20] H. H. Ghouz, "Novel Compact and Dual-Broadband Microstrip MIMO Antennas for Wireless Applications," *Progress In Electromagnetics Research B*, vol. 63, pp. 107–121, Dec. 2015, doi: 10.2528/PIERB15051304.
- [21] A. A. Asaker, R. S. Ghoname, and A.-E. H. Zekry, "Design of a Planar MIMO Antenna for LTE-Advanced," *International Journal of Computer Applications*, vol. 115, pp. 27–33, 2015.